Research Article

Theorems and Application of Local Activity of CNN with Five State Variables and One Port

Gang Xiong,[1] Xisong Dong,[1] Li Xie,[2] and Thomas Yang[3]

[1] *State Key Laboratory of Management and Control for Complex Systems, Institute of Automation, Chinese Academy of Sciences, Beijing 100190, China*
[2] *Department of Information Science and Electronics Engineering, Zhejiang University, Hangzhou 310027, China*
[3] *The Department of Electrical, Computer, Software, and Systems Engineering, Embry-Riddle Aeronautical University, Daytona Beach, FL 32114, USA*

Correspondence should be addressed to Xisong Dong, dongcomic04@163.com

Coupled nonlinear dynamical systems have been widely studied recently. However, the dynamical properties of these systems are difficult to deal with. The local activity of cellular neural network (CNN) has provided a powerful tool for studying the emergence of complex patterns in a homogeneous lattice, which is composed of coupled cells. In this paper, the analytical criteria for the local activity in reaction-diffusion CNN with five state variables and one port are presented, which consists of four theorems, including a serial of inequalities involving CNN parameters. These theorems can be used for calculating the bifurcation diagram to determine or analyze the emergence of complex dynamic patterns, such as chaos. As a case study, a reaction-diffusion CNN of hepatitis B Virus (HBV) mutation-selection model is analyzed and simulated, the bifurcation diagram is calculated. Using the diagram, numerical simulations of this CNN model provide reasonable explanations of complex mutant phenomena during therapy. Therefore, it is demonstrated that the local activity of CNN provides a practical tool for the complex dynamics study of some coupled nonlinear systems.

1. Introduction

Coupled nonlinear dynamical systems have been widely studied in recent years. However, the dynamical properties of these systems are difficult to deal with. Although the research on emergence and complexity has gained much attention during the past decades, the determination, prediction, and control of the complex patterns generated from high-dimensional coupled nonlinear systems are still far from perfect. Nature abounds with complex patterns and structures emerging from homogeneous media, and the local activity is the origin of these complexities [1, 2]. The cellular neural network (CNN), firstly introduced by Chua and Yang [3] as an implementable alternative to fully connected Hopfield neural network, has been widely studied for image processing, robotic, biological versions, and higher brain functions, and so on [3]. Many of the coupled nonlinear systems can be modeled and studied via the CNN paradigm [4]. The local activity proposed by Chua asserts that a wide spectrum of complex behaviors may exist if the cell parameters of the corresponding CNN are chosen in or nearby the edge of chaos [2, 4]. There have been quite a few new methods developed for complex systems [5–8], and local activity has attracted the attention of many researchers. Now, local activity has been successfully applied to the research of complex patterns generated from several CNNs in physical, biological, and chemical domains, such as Fitzhugh-Nagumo equation [9], Brusselator equation [10], Gierer-Meinhart equation [11], Oregonator equation [12], Hodgkin-Huxley equation [13], Van Der Pol equation [14], the biochemical model [15], coupled excitable cell model [16], tumor growth and immune model [17], Lorenz model [18], advanced image processing [19], Rossler equation [20], images analysis [21, 22], data prediction [23], neutron transport equation [24], vision safety [25], retinomorphic model [26], and theory research [27–30], and so forth.

Although Chua presents the main theorem of local activity at a cell equilibrium point [1, 2], it is actually difficult to "test" directly the complex patterns of the high-dimensional coupled nonlinear systems, since the theorem contains no recipe for finding whether a variable actually exists or not. It is necessary to develop some mathematical criteria according to the numbers of the variables and ports; that is the topic addressed in this paper.

The remaining of this paper is organized as follows. The local activity of CNN is introduced in Section 2. A set of theorems for testing the local activity of reaction-diffusion CNN with five state variables and one port are set up in Section 3. As an application of the theorems, a coupled reaction-diffusion CNN of hepatitis B Virus (HBV) mutation-selection model is introduced, aiming at describing HBV mutation in the therapeutic process. The bifurcation diagrams of this CNN are developed and some numerical simulations are presented in Section 4. Concluding remarks are given in Section 5.

2. Local Activity Theory of CNN

The CNN architecture is composed of a two-dimensional $M \times N$ array of cells. Each cell is denoted by $C(i, j)$, where $i = 1, 2, \ldots, M$, $j = 1, 2, \ldots, N$. The dynamics of each cell is given by the equation:

$$\dot{x}_{ij} = -x_{ij} + \sum_{k=-r}^{r} \sum_{l=-r}^{r} a_{kl} y_{i+k\ j+l} + \sum_{k=-r}^{r} \sum_{l=-r}^{r} b_{kl} u_{i+k\ j+l} + z_{ij}, \tag{1}$$

where x_{ij}, y_{ij}, u_{ij} are the state, output, and input variables of the cell, respectively. $a_{k,l}$, $b_{k,l}$, z_{ij} are the elements of the A-template, the B-template, and threshold, respectively. r is the radius of influence sphere. The output y_{ij} is the piecewise linear function given by

$$y_{i,j} = \frac{1}{2}\left(\left|x_{i,j} + 1\right| - \left|x_{i,j} - 1\right|\right), \tag{2}$$
$$i = 1, 2, \ldots, M;\ j = 1, 2, \ldots, N.$$

Clearly, CNN with different template elements may have different functions.

A vast majority of active homogeneous media that are known to exhibit complexity are modeled by a reaction-diffusion partial differential equation (PDE):

$$\frac{\partial x_i}{\partial t} = f_i(X) + D_i\left(\frac{\partial^2 x_i}{\partial x^2} + \frac{\partial^2 x_i}{\partial y^2} + \frac{\partial^2 x_i}{\partial z^2}\right), \quad i = 1, 2, \ldots, n, \tag{3}$$

where $X = (x_1, x_2, \ldots x_n)$ is state variables, (x, y, z) is spatial coordinates, $f_i(x_1, x_2, \ldots, x_n)$ is a coupled nonlinear vector function called the kinetic term, and $D_1, D_2, \ldots, D_n$ are constants called diffusion coefficients. Replacing the Laplace in above formulation by its discrete version yields

$$\frac{\partial^2 x_i}{\partial x^2} + \frac{\partial^2 x_i}{\partial y^2} + \frac{\partial^2 x_i}{\partial z^2} \longrightarrow \nabla^2 X_{\alpha,\beta,\gamma}, \tag{4}$$

where

$$\left(\nabla^2 X_{\alpha,\beta,\gamma}\right)_i$$
$$= x_i(\alpha - 1, \beta, \gamma) + x_i(\alpha + 1, \beta, \gamma) + x_i(\alpha, \beta - 1, \gamma)$$
$$+ x_i(\alpha, \beta + 1, \gamma) + x_i(\alpha, \beta, \gamma - 1)$$
$$+ x_i(\alpha, \beta, \gamma + 1) - 6x_i(\alpha, \beta, \gamma). \tag{5}$$

Chua et al. have introduced reaction-diffusion CNN equations:

$$\dot{X}_{\alpha,\beta,\gamma} = f\left(X_{\alpha,\beta,\gamma}\right) + D\nabla^2 X_{\alpha,\beta,\gamma}, \tag{6}$$

where $D = \operatorname{diag}(D_1, D_2, \ldots D_n)$, $\dot{X}_{\alpha,\beta,\gamma}$ denotes the state variable located at a point in three-dimensional space with spatial coordinates. Chua refers to the process of transforming a PDE into a reaction-diffusion CNN [2].

From Chua and his collaborators' point, PDEs are merely mathematical abstractions of nature, and the concept of a continuum is in fact an idealization of reality. Even the collection of all electrons in a solid does not form a continuum, because much volume separating the electrons from the nucleus represents a vast empty space [2]. Reaction-diffusion CNNs have been used to model some phenomena with important practical backgrounds, which were described by PDEs.

Generally speaking, in a reaction-diffusion CNN, every cell has n state variables, but only m ($m \leq n$) state variables couple directly to their nearest neighbors via "reaction-diffusion". Consequently, each cell has the following state equations:

$$\dot{V}_a = f_a(V_a, V_b) + I_a,$$
$$\dot{V}_b = f_a(V_a, V_b), \tag{7}$$

where

$$V_a = [V_1, V_2, \ldots, V_m]^{\mathrm{T}}, \quad V_b = [V_{m+1}, V_{m+2}, \ldots, V_n]^{\mathrm{T}},$$
$$f_a = [f_1(V_a, V_b), f_2(V_a, V_b), \ldots, f_m(V_a, V_b)]^{\mathrm{T}},$$
$$f_b = [f_{m+1}(V_a, V_b), f_{m+2}(V_a, V_b), \ldots, f_n(V_a, V_b)]^{\mathrm{T}},$$
$$I_a = [D_1 \nabla^2 V_1, D_2 \nabla^2 V_2, \ldots, D_m \nabla^2 V_m]^{\mathrm{T}}. \tag{8}$$

The cell equilibrium point $Q_i = (V_a^i, V_b^i)(\in \mathbb{R}^n)$ of equation (7) can be determined via

$$f_a(V_a, V_b) = 0,$$
$$f_b(V_a, V_b) = 0. \tag{9}$$

The Jacobian matrix at the equilibrium point Q_i has the following form:

$$J(Q_i) = [a_{kl}(Q_i)]_{n \times n} = \begin{bmatrix} A_{aa}(Q_i) & A_{ab}(Q_i) \\ A_{ba}(Q_i) & A_{bb}(Q_i) \end{bmatrix}, \tag{10}$$

where $A_{kl}(Q_i)$ are called cell parameters and

$$
A_{aa}(Q_i) = \begin{bmatrix} \dfrac{\partial f_1}{\partial V_1} & \cdots & \dfrac{\partial f_1}{\partial V_m} \\ \vdots & \ddots & \vdots \\ \dfrac{\partial f_m}{\partial x_1} & \cdots & \dfrac{\partial f_m}{\partial x_m} \end{bmatrix},
$$

$$
A_{ab}(Q_i) = \begin{bmatrix} \dfrac{\partial f_1}{\partial V_{m+1}} & \cdots & \dfrac{\partial f_1}{\partial V_n} \\ \vdots & \ddots & \vdots \\ \dfrac{\partial f_m}{\partial x_{m+1}} & \cdots & \dfrac{\partial f_m}{\partial x_n} \end{bmatrix},
$$

$$
A_{ba}(Q_i) = \begin{bmatrix} \dfrac{\partial f_{m+1}}{\partial V_1} & \cdots & \dfrac{\partial f_{m+1}}{\partial V_m} \\ \vdots & \ddots & \vdots \\ \dfrac{\partial f_n}{\partial x_1} & \cdots & \dfrac{\partial f_n}{\partial x_m} \end{bmatrix},
$$

$$
A_{bb}(Q_i) = \begin{bmatrix} \dfrac{\partial f_{m+1}}{\partial V_{m+1}} & \cdots & \dfrac{\partial f_{m+1}}{\partial V_n} \\ \vdots & \ddots & \vdots \\ \dfrac{\partial f_n}{\partial x_{m+1}} & \cdots & \dfrac{\partial f_n}{\partial x_n} \end{bmatrix}.
$$

$$(11)$$

The local state equations at the cell equilibrium point Q_i are defined via

$$
\begin{aligned}
\dot{V}_a &= A_{aa}V_a + A_{ab}V_b + I_a, \\
\dot{V}_b &= A_{ba}V_a + A_{bb}V_b.
\end{aligned}
\tag{12}
$$

Definition 1.

$$
Y_Q(s) = sI - A_{aa} - A_{ab}(sI - A_{bb})^{-1}A_{ba} \tag{13}
$$

is called the admittance matrix at the cell equilibrium point Q_i.

Lemma 2. *A reaction-diffusion CNN cell is called locally active at the equilibrium point Q_i if and only if, its admittance matrix at Q_i satisfies at least one of the following four conditions [4].*

(1) $Y_Q(s)$ has a pole in $\mathrm{Re}[s] > 0$.

(2) $Y_Q^H(i\omega) = \overline{Y}_Q(i\omega) + Y_Q(i\omega) < 0$ for some $\omega = \omega_0$, where ω_0 is any real number.

(3) $Y_Q(s)$ has a simple pole $s = i\omega_p$ on the imaginary axis, where its associated residue matrix:

$$
k_1 = \begin{cases} \displaystyle\lim_{s \to i\omega_p} \left(s - i\omega_p\right) Y_Q(s), & \text{if } \omega_p < \infty \\ \displaystyle\lim_{\omega_p \to \infty} \dfrac{Y_Q\left(i\omega_p\right)}{i\omega_p}, & \text{if } \omega_p = \infty \end{cases}
\tag{14}
$$

is either a complex number or a negative real number.

(4) $Y_Q(s)$ has a multiple pole on the imaginary axis.

Definition 3. The cell equilibrium point Q_i is called stable if and only if, all the real parts of eigenvalue λ_i of *Jacobian* matrix at the equilibrium point Q_i are negative [2].

Definition 4. A "reaction-diffusion" CNN with n state variables and m ports is said to be operating on the "edge of chaos" with respect to an equilibrium point Q_i if and only if, Q_i is both locally active and stable when $I_a = 0$ [4].

Using the above lemma and definitions, the bifurcation of CNN with respect to an equilibrium point can be divided into three parts: the edge of chaos domains (the locally active and stable domains), the locally active and unstable domains, and the locally passive domains. Numerical simulations indicated that many complex dynamical behaviors, such as oscillatory patterns, chaotic patterns, or divergent patterns, may emerge if the selected cell parameters are located in or nearby the edge of chaos domains.

3. Analytical Criteria for Local Activity of CNN with Five State Variables and One Port

For the reaction-diffusion CNN with five state variables and one port, its local state equations have the form

$$
\begin{aligned}
\dot{V}_a &= A_{aa}V_a + A_{ab}V_b + I_a, \\
\dot{V}_b &= A_{ba}V_a + A_{bb}V_b,
\end{aligned}
\tag{15}
$$

where

$$
V_a = [V_1], \quad V_b = \begin{bmatrix} V_2 & V_3 & V_4 & V_5 \end{bmatrix}^T, \quad I_a = [I_1],
$$

$$
A_{aa} = [a_{11}], \quad A_{ab} = \begin{bmatrix} a_{12} & a_{13} & a_{14} & a_{15} \end{bmatrix},
$$

$$
A_{ba} = \begin{bmatrix} a_{21} & a_{31} & a_{41} & a_{51} \end{bmatrix}^T,
$$

$$
A_{ba} = \begin{bmatrix} a_{21} \\ a_{31} \\ a_{41} \\ a_{51} \end{bmatrix}, \quad A_{bb} = \begin{bmatrix} a_{22} & a_{23} & a_{24} & a_{25} \\ a_{32} & a_{33} & a_{34} & a_{35} \\ a_{42} & a_{43} & a_{44} & a_{45} \\ a_{52} & a_{53} & a_{54} & a_{55} \end{bmatrix}.
$$

$$(16)$$

The corresponding CNN cell admittance matrix $Y_Q(s)$ is given by [1].

$$
\begin{aligned}
Y_Q(s) &= sI - A_{aa} - A_{ab}(sI - A_{bb})^{-1}A_{ba} \\
&= s - a_{11} - \dfrac{T_1 s^3 + K_1 s^2 + L_1 s + \Delta_1}{s^4 + T s^3 + K s^2 + L s + \Delta},
\end{aligned}
\tag{17}
$$

where $T, T_1, K, K_1, L, L_1, \Delta, \Delta_1$ are the parameters of a_{ij}'s.

Theorem 5. *A necessary and sufficient condition for $Y_Q(s)$ to satisfy condition (1) in Lemma 2 is that $\exists s$, such that $g(s) = 0$ ($\mathrm{Re}[s] > 0$), and any one of the following conditions holds.*

(1) $f(s) \neq 0$.

(2) $f(s) = 0$, and $m > n$, where s is m and n orders zero point of $g(s)$ and $f(s)$, respectively, where $f(s) = T_1 s^3 + K_1 s^2 + L_1 s + \Delta_1$, $g(s) = s^4 + T s^3 + K s^2 + L s + \Delta$.

Proof. Obviously proved. □

Denote

$$E = -a_{11}, \quad F = -TT_1 + K_1 - a_{11}(-2K + T^2),$$

$$P = LL_1 - K\Delta_1 - \Delta K_1,$$

$$Q = \Delta_1 + KK_1 - TL_1 - LT_1,$$

$$G = -a_{11}(2\Delta + K^2 - 2LT) - Q,$$

$$H = -a_{11}(L^2 - 2\Delta K) - P,$$

$$I = -a_{11}\Delta^2 - \Delta\Delta_1,$$

$$g(Q) = EQ^4 + FQ^3 + GQ^2 + HQ + I,$$

$$h(\lambda) = -(TT_1 - K_1)\lambda^3 - Q\lambda^2 - P\lambda - \Delta\Delta_1,$$

$$\lambda_{1,2}^* = \frac{-Q \pm \sqrt{Q^2 - 3(TT_1 - K_1)P}}{3(TT_1 - K_1)},$$

$$p = -\frac{3F^2}{16E^2} + \frac{G}{2E}, \quad q = \frac{F^3}{32E^3} - \frac{FG}{8E^2} + \frac{H}{4E},$$

$$w_{1,2} = \frac{-1 \pm i\sqrt{3}}{2},$$

$$D = \frac{q^2}{4} + \frac{p^3}{27}, \quad A_j = \left(-\frac{q}{2} \pm D^{1/2}\right)^{1/3},$$

$$x_1 = A_1 + A_2, \quad x_2 = w_1 A_1 + w_2 A_2,$$

$$x_3 = w_2 A_1 + w_1 A_2, \quad \Omega_i = x_j - \frac{F}{4E}, \quad i = 1, 2, 3.$$

(18)

Theorem 6. *Let the following parameters be defined as in Theorem 5, then $Y_Q^H(iw) < 0$ for some $w = w_0 \in R$ if any one of the following conditions holds.*

(1) $a_{11} > 0$.

(2) $a_{11} = 0, \ TT_1 - K_1 > 0$.

(3) $a_{11} = 0, \ TT_1 - K_1 = 0, \ Q > 0$.

(4) $a_{11} = 0, \ TT_1 - K_1 = 0, \ Q < 0, \ \Delta\Delta_1 > 0$.

(5) $a_{11} = 0, \ TT_1 - K_1 = 0, \ Q < 0, \ P \geq 0, \ \Delta\Delta_1 - P^2/Q/4 > 0, \ \Delta\Delta_1 \leq 0,$

(6) $a_{11} = 0, \ TT_1 - K_1 = 0, \ Q = 0, \ P > 0$.

(7) $a_{11} = 0, \ TT_1 - K_1 = 0, \ Q = 0, \ P \leq 0, \ \Delta\Delta_1 > 0$.

(8) $a_{11} = 0, \ TT_1 - K_1 < 0, \ \Delta\Delta_1 > 0$.

(9) $a_{11} = 0, \ TT_1 - K_1 < 0, \ \Delta\Delta_1 \leq 0, \ and \ \lambda_j^* \geq 0, \ h(\lambda_j^*) < 0, \ for \ j = 1 \ or \ 2$.

(10) $a_{11} < 0, \ D > 0, \ \Omega_1 > 0, \ g(\Omega_1) < 0$.

(11) $a_{11} < 0, \ D < 0, \ and \ \Omega_j \geq 0, \ g(\Omega_j) < 0, \ for \ j = 1, 2 \ or \ 3$.

(12) $a_{11} < 0, \ D = 0, \ p = q = 0, \ g(-F/4E) < 0$.

(13) $a_{11} < 0, \ D = 0, \ q^2/4 = -p^3/27 \neq 0, \ and \ \Omega_j \geq 0, \ g(\Omega_j) < 0, \ for \ j = 1 \ or \ 2$.

Proof. $Y_Q^H(i\omega) = \overline{Y}_Q(i\omega) + Y_Q(i\omega) = 2\,\text{Re}[Y_Q(i\omega)]$, so $Y_Q(i\omega)$ to satisfy condition (2) in Lemma 2 equals to $\text{Re}[Y_Q(i\omega)] < 0$,

$$\text{Re}[Y_Q(i\omega)] = \text{Re}\left[i\omega - a_{11} \right.$$
$$\left. - \frac{T_1(i\omega)^3 + K_1(i\omega)^2 + L_1(i\omega) + \Delta_1}{(i\omega)^4 + T(i\omega)^3 + K(i\omega)^2 + L(i\omega) + \Delta} \right]$$
$$= \frac{E\omega^8 + F\omega^6 + G\omega^4 + H\omega^2 + I}{(\omega^4 - K\omega^2 + \Delta)^2 + (L\omega - T\omega^2)}.$$

(19)

(1) If $a_{11} > 0$, then $\text{Re}[Y_Q(i\omega)] < 0$ when ω is large enough (See (1) of Theorem 6).

(2) If $a_{11} = 0$, then

$$\text{Re}[Y_Q(i\omega)]$$
$$= -\frac{(TT_1 - K_1)\omega^6 + Q\omega^4 + P\omega^2 + \Delta\Delta_1}{(\omega^4 - K\omega^2 + \Delta)^2 + (L\omega - T\omega^2)}.$$

(20)

Let $f(\lambda) = -Q\lambda^2 - P\lambda - \Delta\Delta_1$,

(I) If $TT_1 - K_1 > 0$, then $\text{Re}[Y_Q(i\omega)] < 0$ when ω is large enough (See (2) of Theorem 6).

(II) If $TT_1 - K_1 = 0$, then

(i) If $Q > 0$, then $\text{Re}[Y_Q(i\omega)] < 0$ when ω is large enough (See (3) of Theorem 6).

(ii) If $Q < 0$,

(a) If $\Delta\Delta_1 > 0$, $\exists\omega_0 \in R$, such that $\text{Re}[Y_Q(i\omega_0)] < 0$ (See (4) of Theorem 6).

(b) If $\Delta\Delta_1 \leq 0$, solve $f'(\lambda^*) = 0$, we can get $\lambda^* = -0.5P/Q, f(\lambda^*) = 0.25P^2/Q - \Delta\Delta_1$. Then when $P \geq 0, \Delta\Delta_1 - 0.25P^2/Q > 0$, $\exists\omega_0 > \lambda^*$, such that $\text{Re}[Y_Q(i\omega_0)] < 0$ (See (5) of Theorem 6).

(iii) If $Q = 0$, then $\text{Re}[Y_Q(i\omega)] = -P\omega^2 - \Delta\Delta_1$.

(a) If $P > 0$, then $\text{Re}[Y_Q(i\omega)] < 0$ when ω is large enough (See (6) of Theorem 6).

(b) If $P \leq 0, \Delta\Delta_1 > 0$, then $\exists\omega_0$, such that $\text{Re}[Y_Q(i\omega_0)] = -\Delta\Delta_1 < 0$ (See (7) of Theorem 6).

(III) If $TT_1 - K_1 < 0$, let $h(\lambda) = -(TT_1 - K_1)\lambda^3 - Q\lambda^2 - P\lambda - \Delta\Delta_1$,

(i) If $\Delta\Delta_1 > 0$, then $\exists\omega_0$, such that $\text{Re}[Y_Q(i\omega_0)] < 0$ (See (8) of Theorem 6).

(ii) If $\Delta\Delta_1 \leq 0$, solve $h(\lambda^*) = 0$, we can get

$$\lambda_{1,2}^* = \frac{-Q \pm \sqrt{Q^2 - 3(TT_1 - K_1)P}}{3(TT_1 - K_1)}.$$

(21)

Then, for $i = 1, 2$, if $\lambda_i^* \geq 0, h(\lambda_i^*) < 0$, then $\exists\omega_0$, such that $\text{Re}[Y_Q(i\omega_0)] < 0$ (See (9) of Theorem 6).

(3) If $a_{11} < 0$, let $g(Q) = EQ^4 + FQ^3 + GQ^2 + HQ + I$, then $g'(Q) = 4EQ^3 + 3FQ^2 + 2GQ + H$. Let $x = \Omega + (F/4E)$, then the above becomes $g'(Q) = 4E(x^3 + px + q) = 4Ef(x)$, then x_i, $i = 1, 2, 3$ are the roots of $f(x) = 0$, Ω_i are the roots of $g'(\Omega) = 0$. If any one of the (10)–(13) of Theorem 6 holds, we can get $\text{Re}[Y_Q(i\omega_0)] < 0$.

So, if any one of conditions (1)–(13) holds, $\text{Re}[Y_Q(i\omega_0)] < 0$. $Y_Q(s)$ Satisfies condition (2) in Lemma 2. This completes the proof. □

Theorem 7. *For $j = 1$, or 2, let*

$$w_j = \frac{\left(\sqrt{K + 2\sqrt{\Delta}} + (-1)^j \sqrt{K - 2\sqrt{\Delta}}\right)}{2},$$

$$A_j = L - 3w_j^{*2},$$

$$w_j^* = \sqrt{\frac{\left(K + (-1)^j \sqrt{K^2 - 4\Delta}\right)}{2}}, \quad (22)$$

$$B_j = 2Kw_j^* - 4w_j^{*3}, \qquad A_{1j} = \Delta_1 - K_1 w_j^{*2},$$

$$B_{1j} = L_1 w_j^* - T_1 w_j^{*3}.$$

Then $Y_Q(s)$ satisfies condition (3) of Lemma 2, if any one of the following conditions holds.

(I) $\Delta > 0$, $K > 2\sqrt{\Delta}$, $T = L = 0$, *and any one of the following conditions holds.*

(1) $K_1 w_1^2 - \Delta_1 \neq 0$.
(2) $K_1 w_1^2 - \Delta_1 = 0$, $(L_1 - T_1 w_1^2)(w_2^2 - w_1^2) > 0$.
(3) $K_1 w_2^2 - \Delta_1 \neq 0$.
(4) $K_1 w_2^2 - \Delta_1 = 0$, $(L_1 - T_1 w_2^2)(w_1^2 - w_2^2) > 0$.

(II) $K > 0$, $\Delta_1 \neq 0$, $\Delta = 0$, $L = KT \neq 0$, *and any one of the following conditions holds.*

(1) $T\Delta_1 < 0$.
(2) $T(K - T_1 K) - \Delta_1 + KK_1 \neq 0$.
(3) $T(K - T_1 K) - \Delta_1 + KK_1 = 0$, $T(\Delta_1 - KK_1) + K(L_1 - T_1 K) < 0$.

(III) $\Delta = 0$, $\Delta_1 L > 0$.

(IV) $\Delta < 0$, or $K > 0$, $K^2 - 4\Delta > 0$, *and* $2L = T(K + \sqrt{K^2 - 4\Delta})(K + \sqrt{K^2 - 4\Delta} > 0)$ *or* $2L = T(K - \sqrt{K^2 - 4\Delta})$, $(K - \sqrt{K^2 - 4\Delta} > 0)$ *and any one of the following conditions holds for $j = 1$, or 2.*

(1) $A_j B_{1j} - A_{1j} B_j \neq 0$.
(2) $A_j B_{1j} - A_{1j} B_j = 0$, $A_j A_{1j} - B_j B_{1j} > 0$.

Proof. Let $f(s) = T_1 s^3 + K_1 s^2 + L_1 s + \Delta_1$, $g(s) = s^4 + Ts^3 + Ks^2 + Ls + \Delta$, obviously, ∞ is not a single pole of $Y_Q(s)$ on the imaginary axis.

If $Y_Q(s)$ has a simple pole $s = i\omega$ on the imaginary axis, where its associated residue

$$k_1 = \lim_{s \to i\omega} (s - i\omega) Y_Q(s) = \lim_{s \to i\omega} (s - i\omega) \frac{f(s)}{g(s)} = \left. \frac{f(s)}{g'(s)} \right|_{s=i\omega} \quad (23)$$

is either a complex number or a negative real number, then $k_1 \neq 0$, so $f(s) \neq 0$, which implies that $i\omega$ is not a zero point of $f(s) = 0$, $i\omega$ is not a removed pole of $Y_Q(s)$.

(I) If $Y_Q(s)$ has four poles $s = \pm i\omega_1, \pm i\omega_2$ ($\omega_1 \neq \omega_2 \neq 0$) on the imaginary axis. In this case, $g(s) = (s^2 + \omega_1^2)(s^2 + \omega_2^2) = s^4 + (\omega_1^2 + \omega_2^2)s^2 + \omega_1^2 \omega_2^2$. Hence we obtain $T = L = 0$, $K = \omega_1^2 + \omega_2^2 > 0$, $\Delta = \omega_1^2 \omega_2^2 > 0$. Then, we can get $K + 2\sqrt{\Delta} = (\omega_1 + \omega_2)^2$, $K - 2\sqrt{\Delta} = (\omega_1 - \omega_2)^2$, which implies that $K > 2\sqrt{\Delta}$, $\omega_{1,2} = (\sqrt{K + 2\sqrt{\Delta}} \pm \sqrt{K - 2\sqrt{\Delta}})/2$. So,

$$\lim_{s \to \pm i\omega_1} (s \mp i\omega_1) Y_Q(s) = \frac{w_1(L_1 - T_1 w_1^2) \pm i(K_1 w_1^2 - \Delta_1)}{2w_1(w_2^2 - w_1^2)}, \quad (24)$$

$$\lim_{s \to \pm i\omega_2} (s \mp i\omega_2) Y_Q(s) = \frac{w_2(L_1 - T_1 w_2^2) \pm i(K_1 w_2^2 - \Delta_1)}{2w_2(w_1^2 - w_2^2)}. \quad (25)$$

Then, when condition (I) in Theorem 7 holds, k_1 is a complex number or a negative real number. $Y_Q(s)$ satisfies condition (3) in Lemma 2.

(II) If $Y_Q(s)$ has a simple pole $s = 0$ and two conjugate poles $\pm i\omega$ ($\omega \neq 0$) on the imaginary axis, and another pole is $a \neq 0$.

In this case, it follows that $\Delta = 0$, $\Delta_1 \neq 0$, and $g(s)$ has the form:

$$g(s) = s(s^2 + \omega^2)(s - a)$$
$$= s^4 - as^3 + \omega^2 s^2 - a\omega^2, \quad (26)$$

which implies that $T = -a$, $K = \omega^2 > 0$, $L = -a\omega^2 = KT$, $\Delta = 0$, $\Delta_1 = 0$, Therefore,

$$g(s) = s(s^2 + K)(s + T) \quad (27)$$

(1) The residue of $Y_Q(s)$ at $s = 0$ is

$$\lim_{s \to 0} s Y_Q(s) = \frac{\Delta_1}{(s^2 + K)(s + T)} = \frac{\Delta_1}{KT}. \quad (28)$$

Then, we conclude that if $K > 0$, $\Delta_1 \neq 0$, $\Delta = 0$, $L = KT \neq 0$, $T\Delta_1 < 0$, k_1 is a negative real number. $Y_Q(s)$ satisfies condition (3) in Lemma 2 (See (1) of (II) in Theorem 7).

(2) The residue of $Y_Q(s)$ at $s = \pm i\sqrt{K}$ is

$$\lim_{s \to \pm i\sqrt{K}} \left(s \mp i\sqrt{K}\right) Y_Q(s) = \frac{T(\Delta_1 - KK_1) + K(L_1 - T_1K) \mp i\sqrt{K}(T(L_1 - T_1K) - \Delta_1 + KK_1)}{2K(K + T^2)}. \tag{29}$$

Consequently, we conclude that if (2) or (3) in (II) in Theorem 7 holds, k_1 is either an imaginary number or a negative real number. $Y_Q(s)$ satisfies condition (3) in Lemma 2.

(III) If $Y_Q(s)$ has a simple pole $s = 0$ on the imaginary axis, and the other poles are a_i, $\text{Re}[a_i] \neq 0$, $i = 1, 2, 3$, it follows that $\Delta_1 \neq 0, \Delta = 0$, and $g(s)$ has the form

$$\begin{aligned} g(s) &= s(s - a_1)(s - a_2)(s - a_3) \\ &= s(s^3 - (a_1 + a_2 + a_3)s^2 \\ &\quad + (a_1a_2 + a_1a_3 + a_2a_3)s - a_1a_2a_3). \end{aligned} \tag{30}$$

Therefore we obtain that $\Delta = 0$, $T = -(a_1 + a_2 + a_3)$, $K = a_1a_2 + a_1a_3 + a_2a_3$, $L = -a_1a_2a_3 \neq 0$, hence the reside of $Y_Q(s)$ at $s = 0$ is

$$\lim_{s \to 0} s Y_Q(s) = \frac{\Delta_1}{a_1a_2a_3} = -\frac{\Delta_1}{L}. \tag{31}$$

Then, when $\Delta = 0$, $\Delta_1 L > 0$, k_1 is a negative real number. $Y_Q(s)$ satisfies condition (3) in Lemma 2 (See (III) of Theorem 7).

(IV) If $Y_Q(s)$ has two conjugate poles $\pm i\omega(\omega > 0)$ on the imaginary axis, and the other poles are $\text{Re}[a] \neq 0$, $\text{Re}[b] \neq 0$. In this case, $g(s)$ has the form

$$\begin{aligned} g(s) &= (s - a)(s - b)(s + \omega^2) \\ &= s^4 - (a + b)s^3 + (ab + \omega^2)s^2 \\ &\quad - (a + b)\omega^2 s + ab\omega^2. \end{aligned} \tag{32}$$

Therefore, we obtain that $T = -(a + b)$, $K = ab + \omega^2$, $L = -(a + b)\omega^2$, $\Delta = ab\omega^2 \neq 0$. Then, $ab = K - \omega^2$, $\Delta = (K - \omega^2)\omega^2 \Leftrightarrow \omega^4 - K\omega^2 + \Delta = 0$. Solving it, we have

$$\omega_j^* = \sqrt{\frac{K \pm \sqrt{K^2 - 4\Delta}}{2}}, \quad j = 1, 2. \tag{33}$$

It implies that $\Delta < 0$ or $K > 0$, $K^2 - 4\Delta \geq 0$, and $T = -(a + b) = L/\omega^2$. Then, the residue of $Y_Q(s)$ at $s = \pm\omega_j^*$ is

$$\begin{aligned} &\lim_{s \to \pm i\omega_j^*} \left(s \mp i\omega_j^*\right) Y_Q(s) \\ &= \frac{-\left(A_{1j}A_j + B_{1j}B_j\right) \pm i\left(A_{1j}B_j - A_jB_{1j}\right)}{A_j^2 + B_j^2}. \end{aligned} \tag{34}$$

Hence, if condition (IV) in Theorem 7 holds, $k_1 < 0$ or it is an imaginary number. $Y_Q(s)$ satisfies condition (3) in Lemma 2.

Therefore, when any one of conditions (I)–(IV) holds, $Y_Q(s)$ satisfies condition (3) in Lemma 2. This completes the proof. □

Theorem 8. $Y_Q(s)$ *has a multiple pole on the imaginary axis if any one of the following conditions holds.*

(I) $\Delta = L = 0$, $\Delta_1 \neq 0$.

(II) $\Delta = L = K = 0$, *and* $\Delta_1 \neq 0$ *or* $L_1 \neq 0$.

(III) $\Delta = L = K = T = 0$, *and* $\Delta_1 \neq 0$ *or* $L_1 \neq 0$ *or* $K_1 \neq 0$.

(IV) $T = L = 0$, $K > 0$, $\Delta = (K/2)^2$, *and any one of the following conditions holds.*

(1) $2\Delta_1 \neq KK_1$.

(2) $2L_1 \neq KT_1$.

Proof. Let $f(s) = T_1s^3 + K_1s^2 + L_1s + \Delta_1$, $g(s) = s^4 + Ts^3 + Ks^2 + Ls + \Delta$. Obviously, when the conditions (I)–(III) hold, 0 is the multiply poles of $Y_Q(s)$.

If $Y_Q(s)$ has two multiply nonzero poles $\pm i\omega$ ($\omega > 0$), then $g(s)$ has the form:

$$g(s) = (s^2 + \omega^2)^2 = s^4 + 2\omega^2 s^2 + \omega^4, \tag{35}$$

which implies that $T = L = 0$, $K = 2\omega^2 > 0$, $\Delta = \omega^4 = (K/2)^2 > 0$.

If $\pm i\omega$ are the multiply poles of $Y_Q(s)$, then $f(i\omega) \neq 0$ where

$$\begin{aligned} f(\pm i\omega) &= (\Delta_1 - K_1\omega^2) \pm i\omega(L_1 - T_1\omega^2) \\ &= \left(\Delta_1 - \frac{KK_1}{2}\right) \pm i\omega\left(L_1 - \frac{T_1K}{2}\right). \end{aligned} \tag{36}$$

Obviously, when any one of (1)-(2) of (IV) in Theorem 8 holds, $f(i\omega) \neq 0$, any one of $\pm i\omega$ is a multiply pole of $Y_Q(s)$.

So, when any one of condition (I)–(IV) holds, $Y_Q(s)$ satisfies condition (4) in Lemma 2. This completes the proof.

When any one of Theorems 5–8 holds, $Y_Q(s)$ satisfies Lemma 2, which implies that the reaction-diffusion CNN with five state variables and one port at the equilibrium point is active.

These theorems can be implemented by a computer program for calculating the bifurcation diagram of the general corresponding CNN to determine emergence of complex dynamic patterns of the corresponding CNN. □

TABLE 1: Cell parameters and correspongding dynamic properties of the reaction-diffusion CNN of HBV mutation-selection of HBV infection.

| No.	u	k	Equilibrium point	Eigenvalues	Dynamic pattern
1	2	1.0	20,0,0,19,98	$69.4396, 29.8638, -0.0090, -33.3646, -71.9897$	Convergent, divergent
2	2	3.0	20,0,0,20,98	$-0.0097, 53.0149, 69.4400, -56.5150, -71.9902$	Convergent, divergent
3	2	4.9	20,0,0,20,98	$-0.0098, 68.2343, 69.4485, -71.6962, -72.0368$	Convergent, divergent
4	2	5.1	20,20,50,0,0	$-0.2043 \pm 0.3878i, -0.0000, -2.6014, -2.5000$	Convergent
5	2	10	10,20,99,0,0	$-2.7130, -0.3935 \pm 0.4583i, -0.2192, -2.2808$	Convergent
6	2	24	4,20,239,0,0	$-3.2812, -0.8094 \pm 0.2709i, -0.3768, -2.1232$	Convergent
7	2	39	3,20,389,0,0	$-4.4393, -1.2723, -0.6884, -0.4059, -2.0941$	Convergent
8	5	1.0	50,0,0,19,38	$67.9709, 28.4103, -0.0075, -34.9127, -73.5210$	Convergent, divergent
9	5	3.0	50,0,0,19,38	$-0.0092, 51.5420, 67.9713, -58.0426, -73.5215$	Convergent, divergent
10	5	4.9	50,0,0,19,38	$-0.0095, 66.7552, 67.9801, -73.2207, -73.5651$	Convergent, divergent
11	5	5.1	49,19,19,0,0	$-0.0920 \pm 0.2787i, -0.0092, -5.5160, -5.4909$	Convergent
12	5	10	25,19,39,0,0	$-0.1829 \pm 0.3778i, -0.2375, -5.5343, -5.2625$	Convergent
13	5	24	10,20,95,0,0	$-5.5708, -0.4446 \pm 0.4784i, -0.3915, -5.1085$	Convergent
14	5	39	6,20,155,0,0	$-5.6298, -0.7151 \pm 0.4210i, -0.4343, -5.0657$	Convergent
15	9	1.0	90,0,0,18,20	$66.0620, 26.5823, -0.0055, -37.0867, -75.6121$	Convergent, divergent
16	9	3.0	90,0,0,18,20	$-0.0085, 49.6418, 66.0624, -60.1432, -75.6126$	Convergent, divergent
17	9	4.9	90,0,0,18,20	$-0.0091, 64.8330, 66.0717, -75.3029, -75.6527$	Convergent, divergent
18	9	5.1	88,18,10,0,0	$-0.0531 \pm 0.2110i, -0.0106, -9.5037, -9.4894$	Convergent
19	9	10	45,19,21,0,0	$-0.1047 \pm 0.2973i, -0.2431, -9.5106, -9.2569$	Convergent
20	9	24	19,20,52,0,0	$-0.2481 \pm 0.4288i, -9.5339, -0.3897, -9.1103$	Convergent
21	9	39	12,20,86,0,0	$-0.4014 \pm 0.4931i, -9.5671, -0.4300, -9.0700$	Convergent
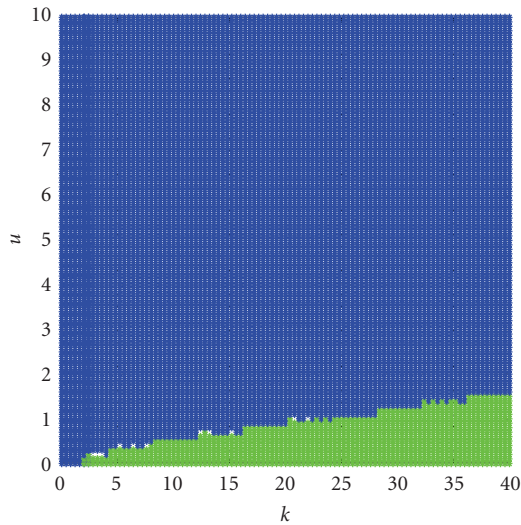
FIGURE 1: Bifurcation diagrams of equation (38) at the equilibrium points Q_1 at $k \in [0, 40]$, $u \in [0, 10]$.
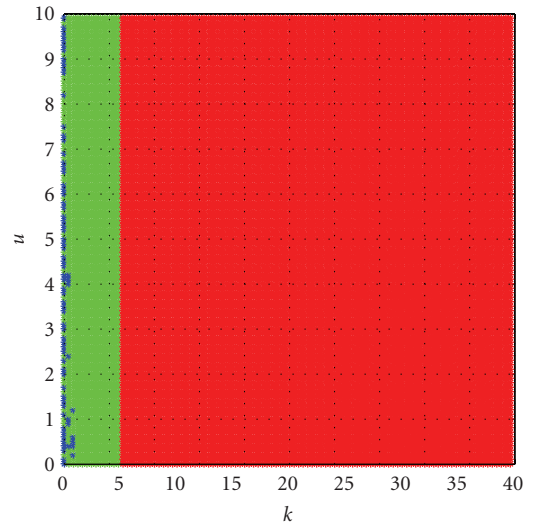
FIGURE 2: Bifurcation diagrams of equation (38) at the equilibrium points Q_2 at $k \in [0, 40]$, $u \in [0, 10]$.

4. Analysis and Simulations of Reaction-Diffusion CNN of HBV Mutation-Selection Model

Life systems consist of locally coupled homogeneous media. Mostly, dynamics of life systems are suitable to be described via locally connected reaction-diffusion CNNs. It may be expected that reaction-diffusion CNN will become a promising candidate for modeling life phenomena.

In Chapter 11 "Timing the emergence of resistance" (Page 110) of the book "Virus dynamic: mathematical principles of immunology and virology" (Oxford university press),

(a)

(b)

- Infected by normal virus
- Infected by mutant virus

(c)

- Normal virus
- Mutant virus

(d)
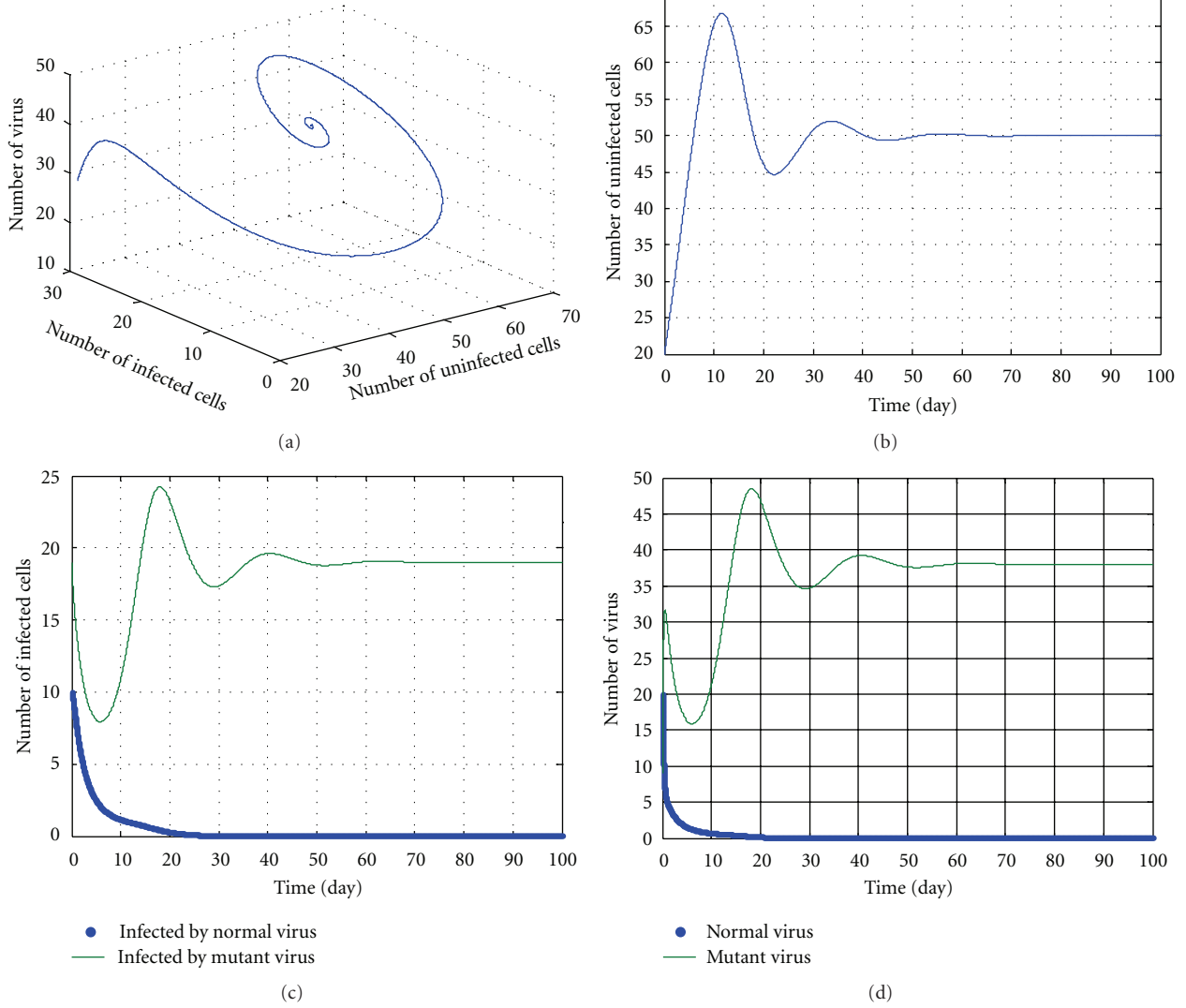
FIGURE 3: The kinetic trajectories of equation (37) when $u = 5$, $k = 3$.

Nowak et al. proposed a mathematical model which describes the mutation selection of HBV infection during the therapy [31]:
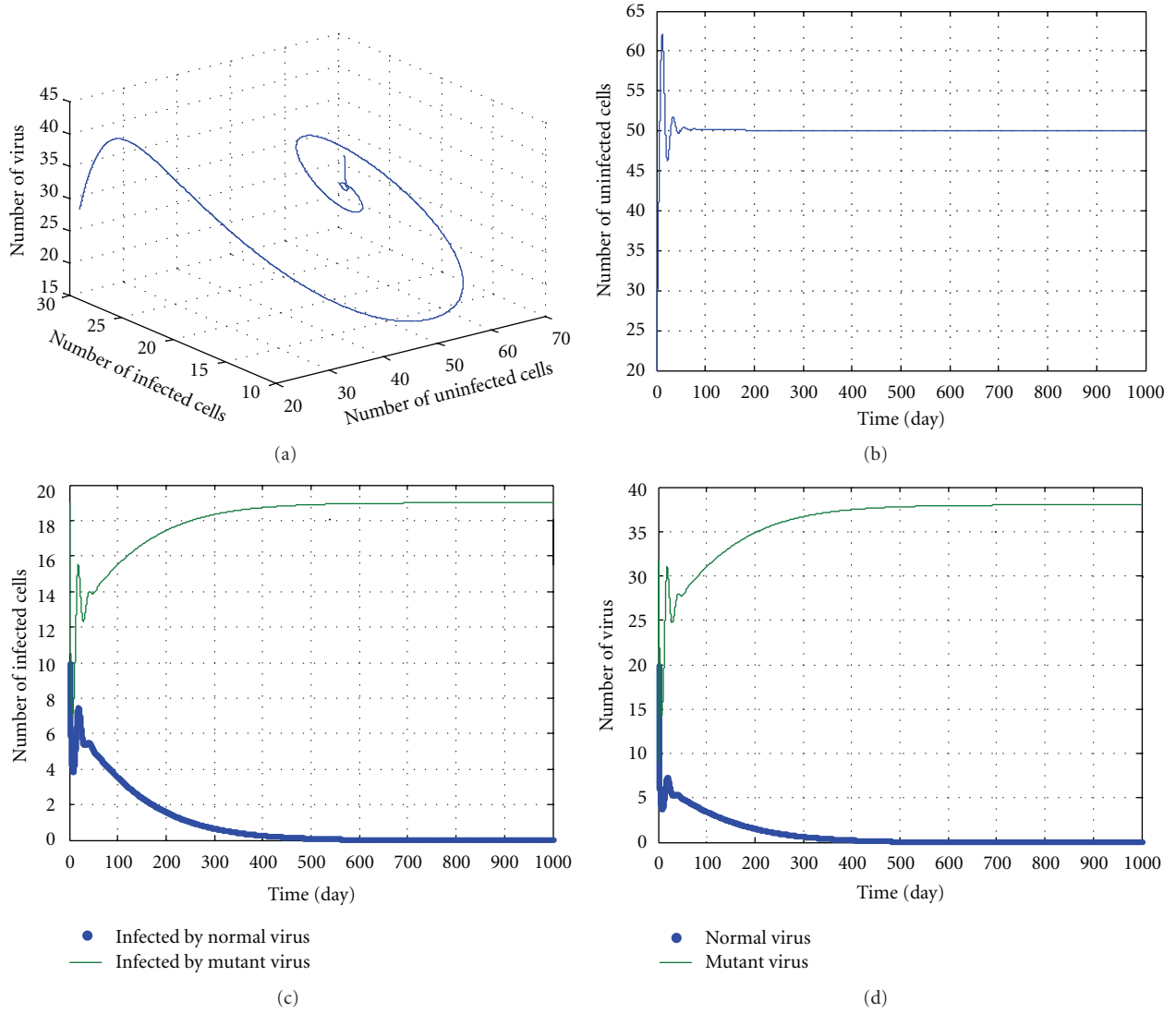
$$\frac{dx}{dt} = \lambda - dx - bvx - b_n x v_n,$$

$$\frac{dy}{dt} = b(1 - e)vx - ay,$$

$$\frac{dv}{dt} = ky - uv, \qquad (37)$$

$$\frac{dy_n}{dt} = bevx + b_n x v_n - a y_n,$$

$$\frac{dv_n}{dt} = k_n y_n - u v_n,$$

where the five variables—x, y, v, y_n, v_n represent the numbers of uninfected cells, infected cells infected by normal virus, normal virus, infected cells infected by mutated virus, and mutant viruses, respectively. λ is the rate of reproduction

of uninfected cells. Uninfected cells die at rate dx and become infected at rate bxv by normal virus and infected at rate $b_n x v_n$ by mutated virus. Infected cells infected by normal and mutated virus are removed at rate ay and ay_n, respectively. Normal virus is produced at rate ky and removed at rate uv, mutated virus is produced at rate $k y_n$ and removed at rate $u v_n$. e is the rate constant describing the probability of mutation of virus (usual 10^{-5}–10^{-3}), a, b, b_n, d, e, k, k_n, u, λ are positive constants. The model was briefly analyzed in Nowak's book.

The reaction-diffusion CNN of HBV mutation selection of model has the form:

$$\frac{dx_{ij}}{dt} = \lambda - dx_{ij} - bx_{ij}v_{ij} - b_n x_{ij} v_{nij} + D_1 \nabla^2 x_{ij},$$

$$\frac{dy_{ij}}{dt} = b(1 - e)x_{ij}v_{ij} - a y_{ij},$$

$$\frac{dv_{ij}}{dt} = k y_{ij} - u v_{ij},$$

(a)

(b)

● Infected by normal virus
— Infected by mutant virus

(c)

● Normal virus
— Mutant virus

(d)

FIGURE 4: The kinetic trajectories of equation (37) when $u = 5$, $k = 4.9$.

$$\frac{dy_{nij}}{dt} = bex_{ij}v_{ij} + b_n x_{ij} v_{nij} - a y_{nij},$$

$$\frac{dv_{nij}}{dt} = k_n y_{nij} - u v_{nij},$$

(38)

where $\nabla^2 x_{ij} = x_{i-1j} + x_{i+1j} + x_{ij-1} + x_{ij+1} - 4x_{ij}$.

Let equation (38) be zeros $(D_1 = 0)$ and solve it, we can get the two equilibrium points:

$$Q_1 = \left(\frac{\lambda}{d}, 0, 0, 0, 0 \right),$$

(39)

$$Q_2 = \left(x_0, \frac{u(au - b_n k_n u x_0)(\lambda - dx_0)}{bkx_0(b_n k_n e x_0 + au - k_n x_0)}, \right.$$

$$\frac{(au - b_n k_n u x_0)(\lambda - dx_0)}{bx_0(b_n k_n e x_0 + au - k_n x_0)}, \frac{eu(\lambda - dx_0)}{b_n k_n e x_0 + au - k_n x_0},$$

$$\left. \frac{k_n e(\lambda - dx_0)}{b_n k_n e x_0 + au - k_n x_0} \right),$$

(40)

where $x_0 = au/((1 - e)bk)$ and Q_1, Q_2 stand for the patient's complete recovery and HBV persistent infection, respectively.

Consequently, the Jacobian matrix at the equilibrium point Q_i ($i = 1, 2$) is

$$J(Q_i) = \begin{bmatrix} -d - bv - b_n v_n & 0 & -bx & 0 & -b_n x \\ b(1-e)v & -a & b(1-e)x & 0 & 0 \\ 0 & k & -u & 0 & 0 \\ bev + b_n v_n & 0 & bex & -a & b_n x \\ 0 & 0 & 0 & k_n & -u \end{bmatrix}.$$

(41)

Taking k, u as variables, and $\lambda = 10$, $a = 0.5$, $b = 0.01$, $b_n = 0.005$, $e = 0.0001$, $k_n = 10$, and $d = 0.01$, using Theorems 5–8, we can calculate the bifurcation of the reaction-diffusion CNN model equation (38) at the equilibrium
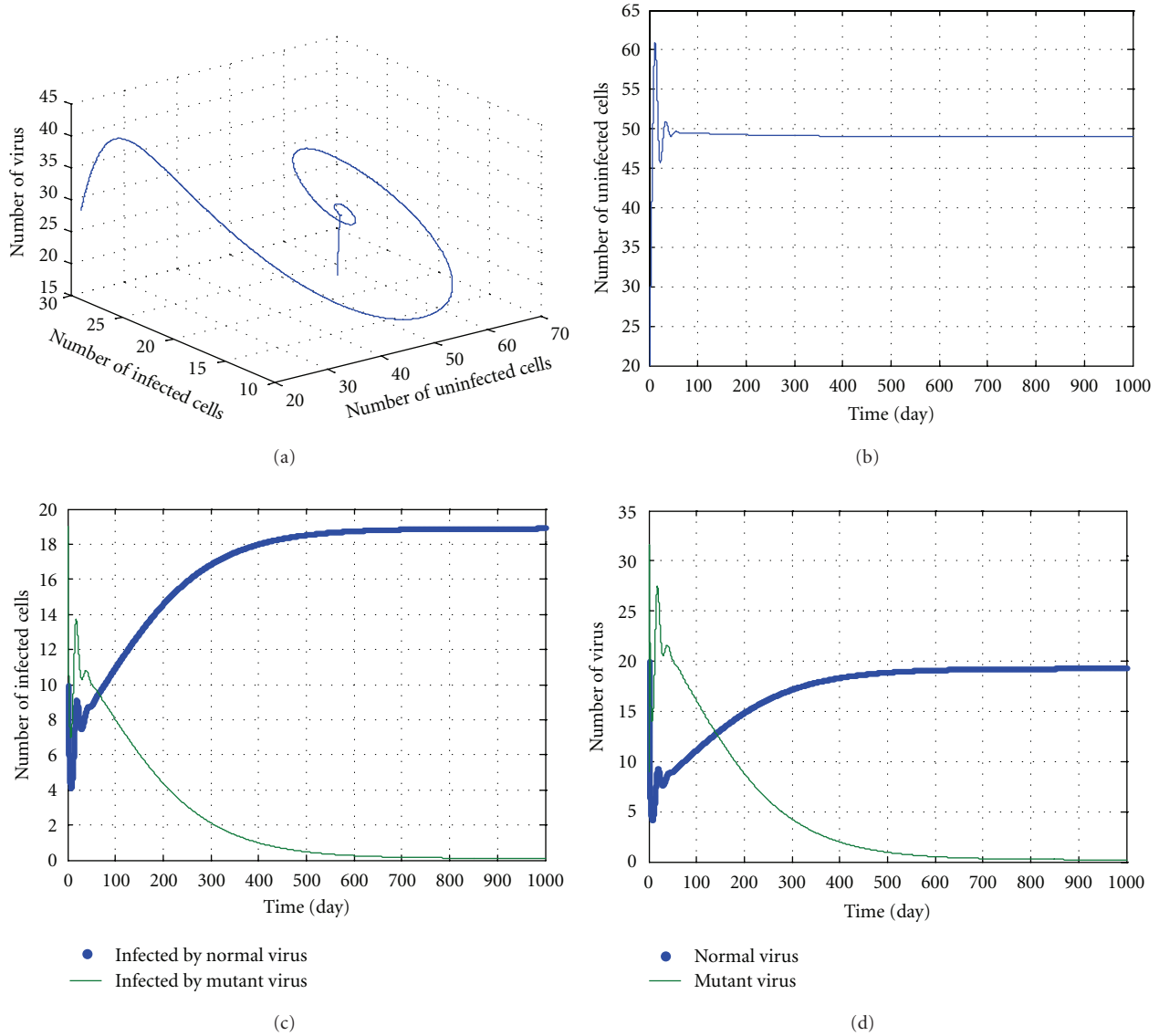
(a)

(b)

●   Infected by normal virus
─   Infected by mutant virus

(c)

●   Normal virus
─   Mutant virus

(d)

FIGURE 5: The kinetic trajectories of equation (37) when $u = 5$, $k = 5.1$.

points Q_1 and Q_2 at $k \in [0, 40]$, $u \in [0, 10]$, see Figures 1 and 2.

In Figures 1 and 2, the domains are coded as follows: edge of chaos (locally active and stable) domain (shown red), locally active and unstable domain (shown green) and locally passive domain (shown blue). From Figure 1(a), we can see that the bifurcation at equilibrium point Q_1 does not exist at the edge of chaos domain.

Take $\lambda = 10$, $k = 0.01$, $a = 0.5$, $b = 0.01$, $b_n = 0.005$, $k_n = 10$, $e = 0.0001$, and $k = 1.0, 3.0, 4.9, 5.1, 10, 24, 39$, $u = 2, 5, 9$, we model the dynamic trajectories of equation (37) using MATLAB, see Table 1.

In the following discussions, we select some parameters in No. 8-14 and $u = 5$, $k = 12.5$. The simulation results are shown in Figures 3, 4, 5, 6, and 7. During the simulation, we reached a new conclusion.

From Table 1 and Figures 3–7, we can conclude that

(I) when k is smaller (less than 5),

    (1) these parameters are located in the green domain (the local and unstable domains);

    (2) regardless of the value of u, the dynamic pattern of equation (37) is convergent or divergent depending on initial values;

    (3) the No. 1, No. 4, and No. 5 variables in equation (37) increase and the No. 2 and No. 3 variables in equation (37) decrease to 0. This means the numbers of the mutant virus and of infected cells infected by mutant virus both increase, and the numbers of normal virus and of the infected cells infected by normal virus both decrease, even to near zero. Also, the

(a)

(b)

(c)

(d)
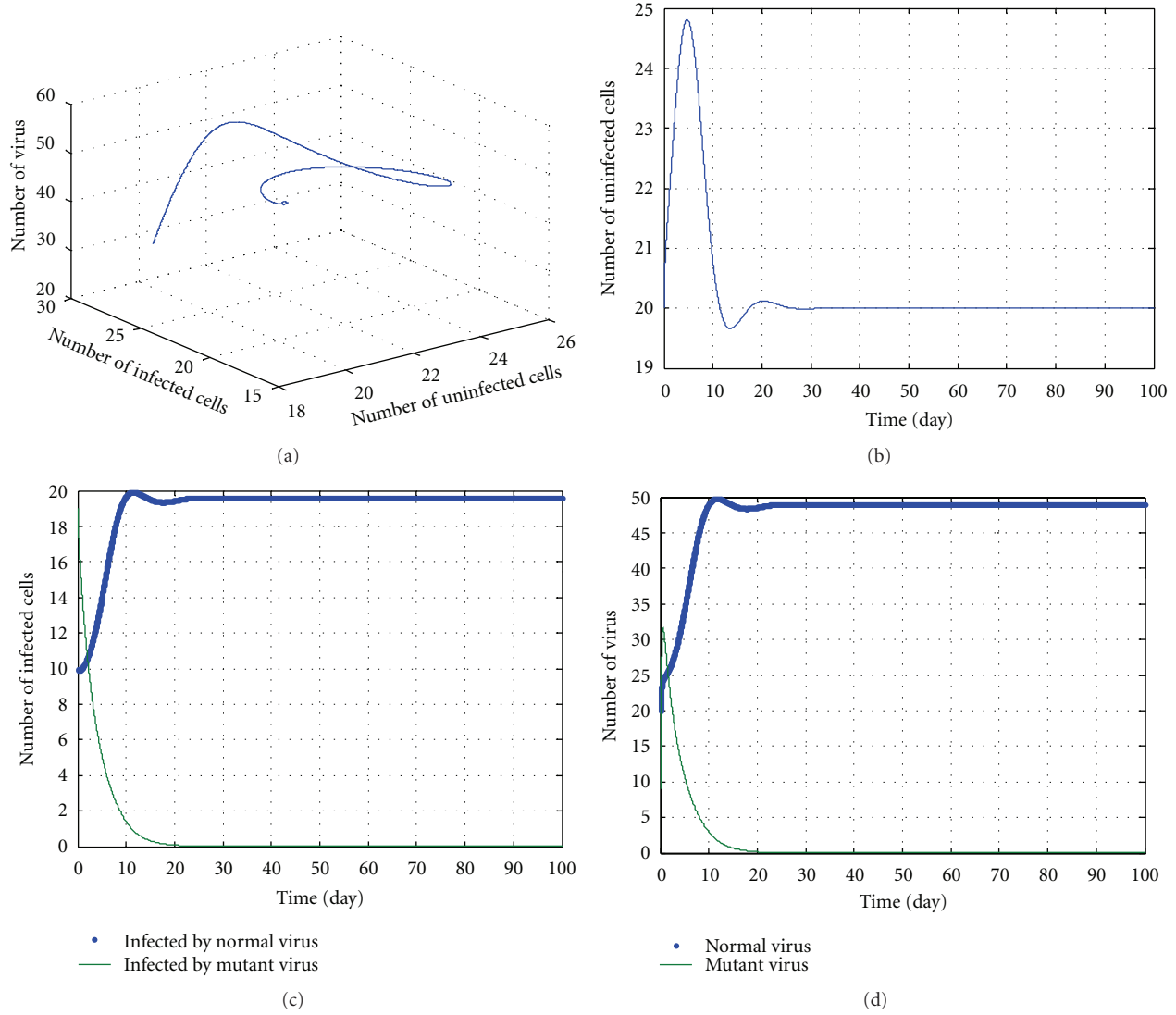
Figure 6: The kinetic trajectories of equation (37) when $u = 5$, $k = 12.5$.

No. 1 variable in equation (37), that is, the number of uninfected cells increases as compared to the initial number. All these indicate that the potency is perfect except for some virus mutation. The potency is ideal.

(II) When k is larger (greater than 5) but less than a threshold value (according to initial values and parameters, for example 12.5 in Figure 6), we can conclude the following.

   (1) These parameters are located in the red domain (edge of chaos).
   (2) Regardless of the value of u, the dynamic pattern of equation (37) is convergent.
   (3) The No. 1, No. 2, and No. 3 variables in equation (37) increase and No. 4 and No. 5 variables decrease to 0. This means that the number of uninfected cells, the numbers of the normal

virus, and of the cells infected by normal virus all increase. Meanwhile, the numbers of the mutant virus and of the cells infected by mutant virus both decrease, even to near zero. All these imply that the drug cannot clean the normal virus, but can destroy the mutant virus and increase the infection cells. The potency is also ideal.

(III) When $k < 40$ and greater than a threshold value (according to initial values and parameters),

   (1) these parameters are located in the red domain (edge of chaos);
   (2) regardless of the u value, the dynamic pattern of equation (37) is convergent;
   (3) The No. 2 and No. 3 variables in equation (37) increase and No. 1, No. 4, and No. 5 variables decrease, which means the numbers of the

(a)

(b)

· Infected by normal virus
— Infected by mutant virus

(c)

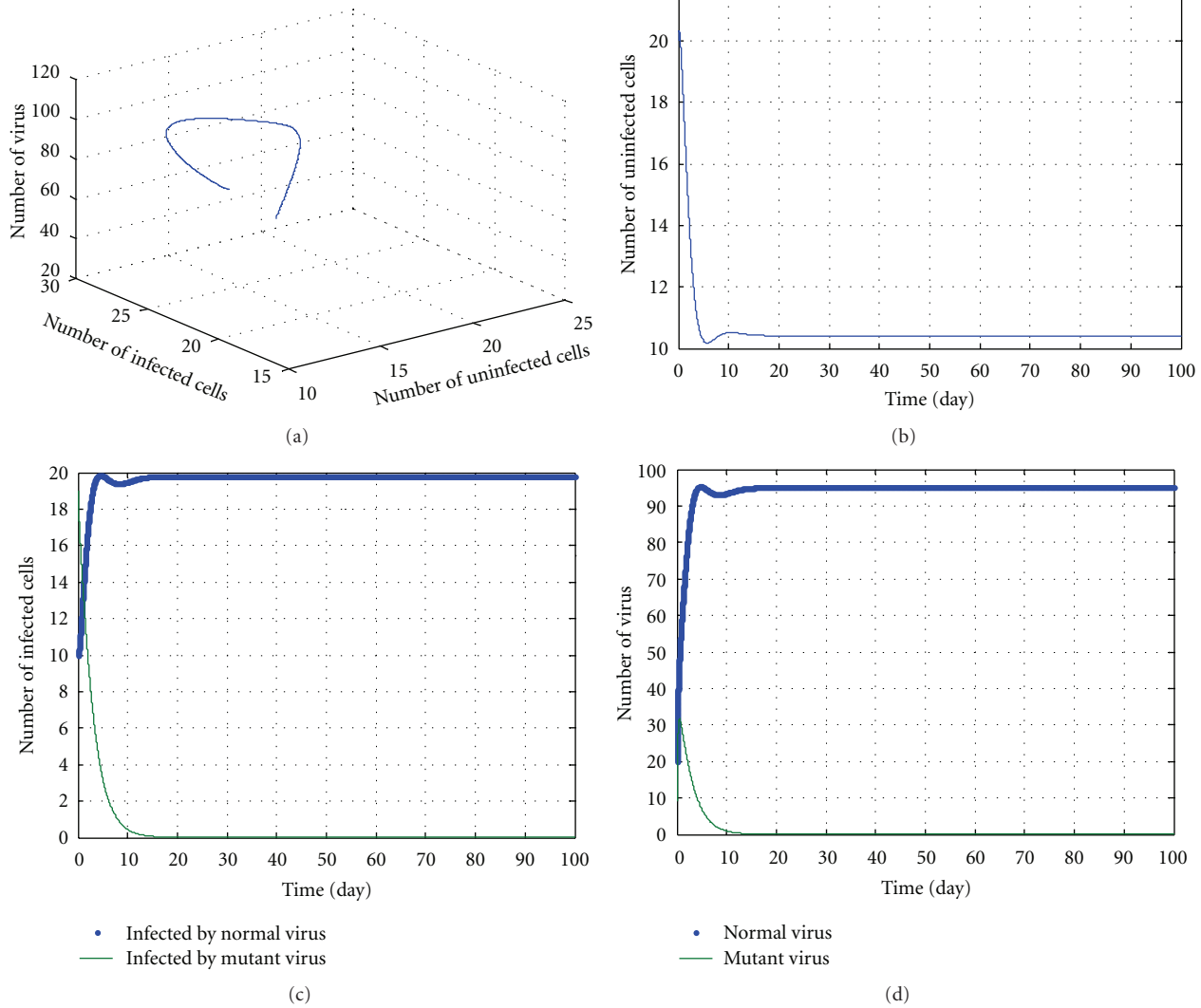· Normal virus
— Mutant virus

(d)

FIGURE 7: The kinetic trajectories of equation (37) when $u = 5$, $k = 24$.

mutant virus and of the uninfected cells decrease, and the number of normal virus increases. These imply that although the drug can prevent the mutation of the HBV effectively, it may destroy uninfected cells and the liver. The potency is not ideal.

5. Conclusions

The local activity of CNN has provided a powerful tool for studying the emergence of complex patterns in a homogeneous lattice formed by coupled cells. Based on the local activity principle, the analytic criteria for the local activity in reaction-diffusion CNN with five state variables and one port are set up. The analytical criteria include four theorems, which provide the inequalities involving the parameters of the CNN. The inequalities can be used for calculating the bifurcation diagram to determine emergence of complex

dynamic patterns of the reaction-diffusion CNN. As an application example, a reaction-diffusion CNN of HBV mutation-selection model is analyzed and simulated, and the bifurcation diagrams are calculated. Numerical simulations show this CNN model may explain certain complex mutant conditions during the therapy. We conclude that the local activity theory provides a practical tool for the study of the complex dynamics of certain coupled nonlinear systems.

Acknowledgment

References

[1] L. O. Chua, "CNN: a version of complexity," *International Journal of Bifurcation and Chaos*, vol. 7, no. 10, pp. 2219–2425, 1997.

[2] L. O. Chua, "Local activity is the origin of complexity," *International Journal of Bifurcation and Chaos*, vol. 15, no. 11, pp. 3435–3456, 2005.

[3] L. O. Chua and L. Yang, "Cellular neural networks: theory and applications," *IEEE Transactions on Circuits and Systems*, vol. 35, no. 10, pp. 1273–1290, 1988.

[4] L. O. Chua, "Passivity and complexity," *IEEE Transactions on Circuits and Systems*, vol. 46, no. 1, pp. 71–82, 1999.

[5] S. Y. Chen, H. Y. Tong, and C. Cattani, "Markov models for image labeling," *Mathematical Problems in Engineering*, vol. 2012, Article ID 814356, 18 pages, 2012.

[6] S. Y. Chen, W. Huang, and C. Cattani, "Traffic dynamics on complex networks: a survey," *Mathematical Problems in Engineering*, vol. 2012, Article ID 732698, 23 pages, 2012.

[7] S. Y. Chen, M. Zhao, G. Wu, C. Yao, and J. Zhang, "Recent advances in morphological cell image analysis," *Computational and Mathematical Methods in Medicine*. In press.

[8] S. Y. Chen, Y. Zheng, C. Cattani, and W. Wang, "Modeling of biological intelligence for SCM system optimization," *Computational and Mathematical Methods in Medicine*, vol. 2012, Article ID 769702, 10 pages, 2012.

[9] R. Dogaru and L. O. Chua, "Edge of chaos and local activity domain of Fitzhugh-Nagumo," *International Journal of Bifurcation and Chaos*, vol. 8, no. 2, pp. 671–693, 1998.

[10] R. Dogaru and L. O. Chua, "Edge of chaos and local activity domain of the Brusselator CNN," *International Journal of Bifurcation and Chaos*, vol. 8, no. 6, pp. 1107–1130, 1998.

[11] R. Dogaru and L. O. Chua, "Edge of chaos and local activity domain of the Gierer-Meinhardt CNN," *International Journal of Bifurcation and Chaos*, vol. 8, no. 12, pp. 2321–2340, 1998.

[12] L. Q. Min, K. R. Crounse, and L. O. Chua, "Analytical criteria for local activity and applications to the oregonator CNN," *International Journal of Bifurcation and Chaos*, vol. 10, no. 1, pp. 25–71, 2000.

[13] L. Q. Min, K. R. Crounse, and L. O. Chua, "Analytical criteria for local activity of reaction-diffusion CNN with four state variables and applications to the Hodgkin-Huxley equation," *International Journal of Bifurcation and Chaos*, vol. 10, no. 6, pp. 1295–1343, 2000.

[14] L. Q. Min and G. Chen, "Local activity of the Van der Pol CNN," *International Journal of Bifurcation and Chaos*, vol. 14, no. 7, pp. 2211–2222, 2004.

[15] L. Q. Min and N. Yu, "Analytical criteria for local activity of CNN with two-port and application to biochemical model," *Journal of University of Science and Technology Beijing*, vol. 7, no. 4, pp. 305–314, 2000.

[16] L. Q. Min and N. Yu, "Some analytical criteria for local activity of two-port CNN with three or four state variables: analysis and applications," *International Journal of Bifurcation and Chaos*, vol. 12, no. 5, pp. 931–963, 2002.

[17] L. Q. Min, J. Wang, X. Dong, and G. Chen, "Some analytical criteria for local activity of three-port CNN with four state variables: analysis and applications," *International Journal of Bifurcation and Chaos*, vol. 13, no. 8, pp. 2189–2239, 2003.

[18] L. Q. Min and N. Yu, "Application of local activity theory of cellular neural network with two ports to the coupled Lorenz-cell model," *Communications in Theoretical Physics*, vol. 37, no. 6, pp. 759–767, 2002.

[19] M. Itoh and L. O. Chua, "Advanced image processing cellular neural networks," *International Journal of Bifurcation and Chaos*, vol. 17, no. 4, pp. 1109–1150, 2007.

[20] Y. Meng, L. Q. Min, and Y. Ji, "Application of local activity theory to rossler CNN model," in *Proceedings of the 9th International Conference for Young Computer Scientists (ICYCS '08)*, pp. 2846–2851, November 2008.

[21] H. Li, X. Liao, C. Li, H. Huang, and C. Li, "Edge detection of noisy images based on cellular neural networks," *Communications in Nonlinear Science and Numerical Simulation*, vol. 16, no. 9, pp. 3746–3759, 2011.

[22] W. Borges Sampaio, E. Moraes Diniz, A. Corrĉa Silva, A. Cardoso de Paiva, and M. Gattass, "Detection of masses in mammogram images using CNN, geostatistic functions and SVM," *Computers in Biology and Medicine*, vol. 41, no. 8, pp. 653–664, 2011.

[23] S. U. Alver, B. Cuma, and U. N. Osman, "Application of cellular neural network (CNN) to the prediction of missing air pollutant data," *Atmospheric Research*, vol. 101, no. 1-2, pp. 314–326, 2011.

[24] A. Pirouzmand and K. Hadad, "Cellular neural network to the spherical harmonics approximation of neutron transport equation in x-y geometry—part I: modeling and verification for time-independent solution," *Annals of Nuclear Energy*, vol. 38, no. 6, pp. 1288–1299, 2011.

[25] A. Grabowski, R. A. Kosiński, and M. Dźwiarek, "Vision safety system based on cellular neural networks," *Machine Vision and Applications*, vol. 22, no. 3, pp. 581–590, 2011.

[26] J. J. Martínez, J. Garrigós, J. Toledo, E. Fernández, and J. Manuel Ferrández, "Implementation of a CNN-based retinomorphic model on a high performance reconfigurable computer," *Neurocomputing*, vol. 74, no. 8, pp. 1290–1297, 2011.

[27] M. Di Marco, M. Grazzini, and L. Pancioni, "Global robust stability criteria for interval delayed full-range cellular neural networks," *IEEE Transactions on Neural Networks*, vol. 22, no. 4, pp. 666–671, 2011.

[28] S. Long and D. Xu, "Stability analysis of stochastic fuzzy cellular neural networks with time-varying delays," *Neurocomputing*, vol. 74, no. 14-15, pp. 2385–2391, 2011.

[29] L. Wan and Q. Zhou, "Attractor and ultimate boundedness for stochastic cellular neural networks with delays," *Nonlinear Analysis. Real World Applications*, vol. 12, no. 5, pp. 2561–2566, 2011.

[30] M. Syed Ali and P. Balasubramaniam, "Global asymptotic stability of stochastic fuzzy cellular neural networks with multiple discrete and distributed time-varying delays," *Communications in Nonlinear Science and Numerical Simulation*, vol. 16, no. 7, pp. 2907–2916, 2011.

[31] M. A. Nowak et al., *Virus Dynamics—Mathematical Principles of Immunology and Virology*, chapter 11, Oxford university press, 2000.